Proceedings of the 2002 IEEE
International Conference on Robotics & Automation
Washington, DC • May 2002

Automated Inspection System Using Range Data

F. Prieto[1], P. Boulanger[2], R. Lepage[3] and T. Redarce[4]

[1] Universidad Nacional de Colombia Sede Manizales, PCI.
Carrera 27 # 64 - 60, Manizales (Caldas), Colombia, fprieto@nevado.manizales.unal.edu.co
[2] Department of Computing Science, University of Alberta, 2-21 Athabasca Hall
Edmonton, Alberta, T6G 2E8, Canada, pierreb@cs.ualberta.ca
[3] ÉTS, Laboratoire d'Imagerie, de Vision et d'Intelligence Artificielle,
1100 rue Notre-Dame Ouest, Montréal, Québec, H3C 1K3, Canada, lepage@livia.etsmtl.ca
[4] INSA, Laboratoire d'Automatique Industrielle,
20 avenue Albert Einstein, 69621 Villeurbanne Cedex, France, redarce@lai.insa-lyon.fr

Abstract— **We propose an automated inspection system of manufactured parts using a cloud of 3D measured points of a part provided by a range sensor, and its CAD model. Inspection consists in verifying the accuracy of a part related to a given set of tolerances. It is thus necessary that the 3D measurements be accurate. In the 3D capture of a part, several sources of error can alter the measured values. So, we have to find and model the most influent parameters affecting the accuracy of the range sensor in the digitalization process. This model is used to produce a sensing plan to acquire accurately the geometry of a part. By using the noise model, we introduce a dispersion value for each 3D point acquired. This value of dispersion is shown as a weight factor in the inspection results.**

Keywords— **Industrial Inspection, CAD-Based Machine Vision, Range sensor, Optimal Sensor Placement, View Planning.**

I. Introduction

CAD/CAM is largely used in industry. After the design and manufacturing of a piece remains a significant task: the *inspection*. Inspection is the process of determining if a product (part or whole) deviates from a given set of specifications (tolerances). Coordinate Measuring Machine (CMM) is the industry standard mechanism for part validation, but in spite of its high accuracy, it has some important limitations such as: the need for mechanical fixturing, low measurement speed, and the need to be programmed as a new part is inspected.

On the other hand, recent advances in non-contact sensor like laser range finder, with significant improvement in speed (about 20000 points/s), allow them to be used in inspection tasks. The disadvantage of the range sensors is their accuracy, largely lower than the CMM accuracy. If one wants to improve the overall accuracy, it is necessary to develop acquisition strategies that optimize the digitalization process. Finally, if the dimensional inspection is relatively simple to realize, it is mandatory however to develop methodologies for geometrical inspection.

In this paper we present an inspection methodology for geometrical tolerances that uses the CAD model of the part and the high accuracy 3D range data obtained after the scanning of the 3D part using an acquisition strategy that optimizes the accuracy.

II. Accuracy of measured points

This section describes the accuracy that can be obtained from the 3D data as a function of the placement of the range camera. The camera, an auto-synchronized range sensor, was developed at National Research Council of Canada [1].

In order to evaluate the accuracy of the cloud of 3D points obtained by the scanning process, we have achieved 128 measurements, each time at different positions for the distance and the orientation of the laser sensor with respect to a reference surface. The measurments were fulfilled after the camera calibration procedure, and the camera placements were chosen close to the calibration ones.

In Figure 1(a), we show the variance (in mm^2) in the axis of the projected beam (z axis) versus the distance (in mm) from the camera to the surface. The dotted curve is a second degree polynomial that best fit the real variances curve. The fitting curve is defined as $Var(d) = 8.86\times10^{-10}\cdot d^2 - 3.47\times10^{-7}\cdot d + 3.81\times10^{-5}$. From Figure 1(a), we can conclude that in spite of oscillations created by speckle effects, the variance has a smaller dispersion when the camera is nearest to the surface. To improve the measurement accuracy by finding the best scanning placements, we define a distance range for the placements as $170mm \leq d \leq 240mm$. For distances smaller than $170mm$, the measurement accuracy is worse, because the laser beam get out of focus.

0-7803-7272-7/02/$17.00 © 2002 IEEE

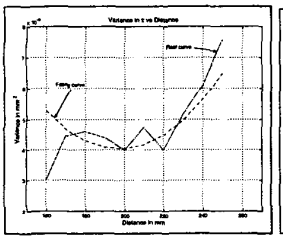

(a) Variance in Z versus distance.

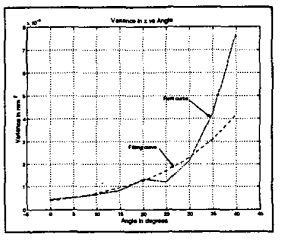

(b) Variance in Z versus incident angle in the direction of the laser sweep.

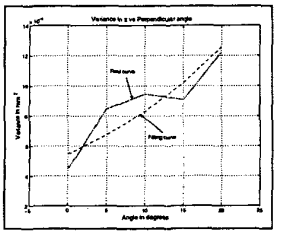

(c) Variance in Z versus incident angle in a perpendicular direction to the laser sweep.

Fig. 1. Variance of the range sensor in the Z direction.

In Figure 1(b), we show the variance (in mm^2) in the laser propagation axis versus the incident angle (in degrees) the laser beam reaches the surface. The dotted curve is an exponential function $Var(\alpha) = 3.77 \times 10^{-6} \cdot e^{6.01 \times 10^{-2} \cdot |\alpha|}$ that best fit the real curve of variances. The incident angle is measured in the same direction as the laser beam sweep. From Figure 1(b), we observe that the smaller dispersion value is produced for an incident angle near to zero degrees, or normal to the surface. For the definition of the best scanning placements, we set the laser beam sweep range as $-35° \leq \alpha \leq 35°$. The range starts at $-35°$ and not $0°$ because we have a symmetrical result when the angle α increases in the opposite direction.

Another parameter which influences the value of the variance is the incident angle in a perpendicular direction from the laser beam sweep (angle (β)). In Figure 1(c), we present the variance (in mm^2) in the axis of the beam projection versus the incident angle β (in degrees). The dotted curve is an exponential function $Var(\beta) = 5.47 \times 10^{-6} \cdot e^{4.15 \times 10^{-2} \cdot |\beta|}$, the best fit of the real variance curve. Similarly as for the angle α, we can conclude from Figure 1(c) that the dispersion is smaller when the incident angle is near to zero, or normal to the surface. For the definition of the best scanning placements, and looking at the behavior of the curve, we have set the laser beam sweep range as $-15° \leq \beta \leq 15°$.

These results confirm that we can improve the accuracy of the data acquisition process by following the previously defined criterions (normal direction, distance). So, in order to be able to achieve inspection tasks, we have implemented an acquisition planning strategy. The strategy improves the 3D data accuracy by finding the optimal camera placement for digitizing the part, using the range for the parameters d, α and β computed in this section.

III. The Acquisition Planning Strategy

The main goal of this strategy is to improve the measurement accuracy of a part. Such a strategy consists in computing the set X of viewpoints x^i in order to obtain a complete and optimal 3D image of the part. We define an optimal 3D image as a 3D cloud acquired by the scanning process in the best accuracy conditions. The resulting 3D image can be used, for instance, in inspection task for verifying the specification of just a few surfaces. The strategy is therefore to find the collection of viewpoints for each surface independently. If one wants to digitize the whole part, he just has to add the complete assemblies X of all the surfaces in the part. In most of the related works [2–4], the acquisition strategy is optimized to have the minimum number of viewpoints to digitize the whole part. In our work [5], the placement strategy optimizes the accuracy of the acquired 3D points and can be applied to a particular surface or to the whole part.

We define a viewpoint as a set of 7 parameters $x^i = \{x, y, z, \phi, \theta, \psi, \gamma\}^i$. Three position parameters (x, y, z) defining the spatial placement of the camera relative to the coordinate system of the part, three orientation parameters (ϕ, θ, ψ) defining the direction of the laser beam, and one parameter γ specifying the angle of the controlled sweep. The set X of viewpoints x^i is defined as $X = \{x^1 x^2 ... x^i ... x^n\}$, with n the minimum number of viewpoints necessary to digitize a simple surface or the whole part.

The system requirements are knowledge of the exact position and orientation of the part and of the CAD model of the part in IGES format. In the IGES CAD model, all the surfaces of the part are defined as parametric NURBS (Non-Uniform Rational B-Splines) surfaces. We use a registration process to determine the placement of the part, as implemented by Moron [6], which relies on the work of Besl and McKay [7]. This process registers an unordered cloud of 3D points of the part with its CAD model. The CAD model is

used not only for the registration process, but also for the search of viewpoints and to resolve the occlusion problem.

We stated that the accuracy of a measured point using an auto-synchronized range sensor (previously calibrated) depends specifically on the scanning distance and on the incidence angle of the laser beam relative to the surface. The measured points are more accurate when the camera is located near the part and when the incidence angle of the laser ray is near to the normal direction of the surface. The strategy searches for viewpoints to digitize the part with the best conditions for accuracy.

The viewpoint issue of the strategy is that inspected surface can be reached by the mechanical support of the camera and is occlusion free. A surface is occluded for a specific viewpoint if any object intersects the laser beam before reaching the target surface. The system works with both simple and complex surfaces. The only geometric constraint imposed to the parts to be digitized is that they are completely contained within the workspace of the camera.

Sensor placement strategy results

We show in Figure 2 some industrial parts that were digitalized with and without the use of the sensor placement strategy. In Figure 3, we show the sensing strategies, issued from the acquisition planning strategy described in [5], for a complete digitalization of the parts. In the Figure 3, the line represents the projection of the laser beam from the viewpoint, where the sensor is placed, to the projected viewpoint on the surface in the optical axis direction. After the registration process of the 3D data with the CAD model of the part, the distance between each 3D point and the nearest point on the CAD model is computed. Table I summarizes the average distance for each part. The average distance for standard digitalization is presented in the column *Stand Dig*. The column *Strat Dig* present the average distance for the digitalization by using the sensor placement strategy. The last column shows the improvement obtained when the strategy is used.

TABLE I
AVERAGE DISTANCE BETWEEN EACH 3D POINT AND THE NEAREST POINT ON THE NURBS SURFACE

Part	Stand Dig	Strat Dig	Improvement
Part 1	$73\mu m$	$48\mu m$	$25\mu m$ (34%)
Part 2	$153\mu m$	$100\mu m$	$53\mu m$ (35%)
Part 3	$99\mu m$	$66\mu m$	$33\mu m$ (33%)

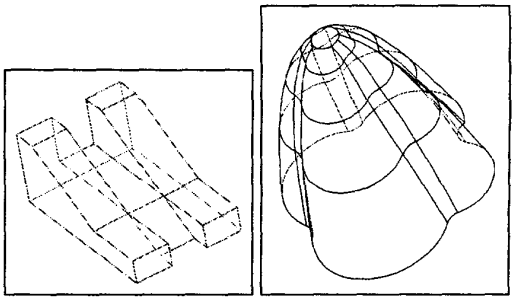

(a) Part 1 (b) Part 2

Fig. 2. Some industrial parts

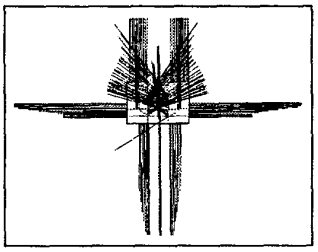

(a) Part 1

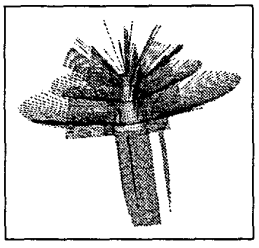

(b) Part 2

Fig. 3. Some sensing strategies

The smallest average distance is obtained for part 1 followed by part 3, all of the parts composed of flat surfaces. For these two parts we obtain an improvement of approximately 33%. For the part 2 the improvement obtained is of 35% but the average distance is $100\mu m$: it represents the largest distance. This result is due to the fact that this part is composed of curved surfaces, and thus the incidence angle of the laser beam is far away from the optimal one.

IV. TOLERANCE INSPECTION

Manufacturing methods are unable to produce parts with perfect shape, size and form. Therefore, given a physical instance of a part, it is possible to measure dimensional or geometric properties, and determine if deviations are within range defined by the tolerance specification. Usually the inspection of a part using 3D range data is done by comparing the CAD model with 3D data after registration [4, 8]. In order to use only the 3D points related to the tolerance specification (points on the reference surface and points on the inspected surface), the 3D cloud is segmented after the registration process [9].

A. The registration method

The registration of two shapes is defined as finding the 3D rigid transformation (rotation + translation) to be applied on one of the shape to bring it into one common cartesian coordinate system with the other one. The registration process relies on the well-known work of Besl and McKay [7] who in 1992 developed a general-purpose representation method for the accurate and computationally efficient registration of 3D shapes, including free-form curves and surfaces. Moron [10] implemented an algorithm for registration between an unordered cloud of 3D points and a CAD model. In the CAD model used, all the surfaces of the part are defined as a parametric NURBS (Non-Uniform Rational B-Splines) surfaces.

B. The segmentation method

In the registration process, we superposed the CAD model with the 3D data of the part. But because we are interested in inspecting some specific surfaces, we need to segment the part into its different surfaces. The segmentation of the 3D cloud is done by computing the distance between every 3D point and all of the surfaces in the CAD model, and by comparing some local geometric properties between each 3D point in the cloud and its closest point on the surface.

C. Geometrical tolerance

The geometrical tolerance is the maximum range in which can vary the geometrical characteristics of form, orientation or position of an element. Figure 4 shows the tolerance specifications (in mm) for part 1.

C.1 Form tolerance

We check form tolerances of a surface by using only the 3D points associated with this surface and obtained from the segmentation process. This subset of 3D points is registered with the CAD model, and the perpendicular distance between each 3D point and the NURBS surfaces is calculated. The distribution of these distances, a gaussian distribution, is used to define the zone of measured tolerance. Indeed, we adjust the average value of the distribution with the NURBS surface (of the CAD model). We place two parallel surfaces to the NURBS surface at a distance $\pm 2\sigma$, then the measured tolerance is equal to: $t_m = 4\sigma$.

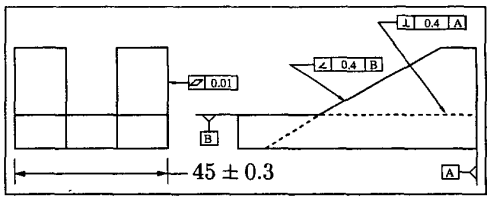

Fig. 4. Tolerance specifications

For form tolerances, we say that surface is in conformity with the specification if the following relation is satisfied: $t_m \leq t_s$, where: t_m is the measured distance between the parallel plans and t_s is the specified tolerance.

C.2 Orientation tolerance

In order to verify the conformity of an orientation tolerance, we must use two subsets of points: S_i associated to the surface to be inspected and S_r associated to the reference surface. The subset S_r is registered with CAD model and the computed rigid transformation is also applied to S_i. The perpendicular distance between each 3D point of S_i and NURBS surface is computed. The distribution of these distances does not have a gaussian form, and thus two points are defined in order to evaluate the zone of measured tolerance. (i) The point p_1 at a distance d_1 from the NURBS surface such that 2.5% of the points in S_i have a distance $d_i \leq d_1$. (ii) The point p_2 at a distance d_2 from the NURBS surface such that 2.5% of the points in S_i have a distance $d_i \geq d_2$. The zone of measured tolerance is then defined as the range between two parallel planes with an orientation related to the reference surface and passing through the points p_1 and p_2. For orientation tolerances, the inspected surface is in conformity with the specification t_s if the following relation is satisfied: $t_m = |d_2 - d_1| \leq t_s$.

C.3 Location tolerance

The location tolerances are controlled similarly to the tolerances of orientation. To ensure the conformity of the surface under inspection, the following relation must be satisfied: $t_{1_s} \leq t_{1_m} < t_{2_m} \leq t_{2_s}$, where: t_{1_s} and t_{2_s} are the distances from the surfaces which define the zone of tolerance specified to the reference, and t_{1_m} and t_{2_m} are the distances from the surfaces which define the zone of tolerance measured to the

real reference (S_r).

D. Nondeterministic inspection

A real image is seldom free from noise, and thus leads to uncertainties in the attributes of the entities resulting from image processing. In the case of 3D images, these entities are the subsets of 3D points (after the segmentation process) and the 3D points themselves. Uncertainty in the entities of the image leads to uncertainty in the inspection tasks. In this section we discuss the effect of this uncertainty in the results of the inspection. We suppose that the range data was obtained by using a strategy detailed in section III.

D.1 Noise model

We have exposed in section II the noise model of the digitalization system. Let $\vec{r}_{ij}$ be the real value of the point (x_i, z_j) on surface, and let $(\hat{x}_i, \hat{z}_j)$ be the acquired value of the point The model for a noisy point measured by the sensor is: $(\hat{x}_i, \hat{z}_j) = (x_i, z_j) + b(x_i, z_j)$.

The noise is described by a probability density function with a gaussian distribution of mean zero and variance σ, as follow:

$$b(\vec{r}) = \frac{1}{(2\pi)^{3/2}\sqrt{|\Sigma|}} exp\left(-\frac{1}{2}(\vec{r}-\vec{s})^{\top}\Sigma^{-1}(\vec{r}-\vec{s})\right),$$

where $\vec{s}$ is a two-dimensional vector corresponding to the point on the NURBS surface nearest to $\vec{r}$, and $\Sigma(\vec{r})$ is the covariance matrix for the point $\vec{r}$.

The properties of the noise function $b(\vec{r})$ can be interpreted geometrically, assigning a constant probability to the intersection of the function $b(\vec{r})$ with an horizontal plane. These intersections form a family of ellipses. When the center of the ellipse coincides with the origin of the reference frame, the form and the orientation are defined completely by Σ. Indeed, the length of the major and minor axes can be calculated easily as the square root of the eigenvalues of Σ. The length of the axes of the dispersion ellipse for the point $\vec{r}$ can then be calculated by:

$$L_{x(z)}(\vec{r}) = \sqrt{\frac{1}{2}(\sigma_{xx(xz)}(\vec{r}) + \sigma_{xz(zz)}(\vec{r}))},$$

where $L_x(\vec{r})$ is the length of the minor axis and $L_z(\vec{r})$ is the length of the major axis, since for the point $\vec{r}$ we know that $\sigma_{zz}(\vec{r}) > \sigma_{xz}(\vec{r})$ (Section II).

D.2 Noise consideration in inspection results

The matrix of covariance Σ is a function of the digitalization parameters such as: the incident angle α, the incident angle β and the distance d from the sensor to the surface.

The form of the variance at the point $\vec{r}$ is an ellipse, the major axis showing the largest dispersion of the point $\vec{r}$. We compute the major axis using $\sigma_{xz}(\vec{r}) = \sigma_{xz}(\alpha)+\sigma_{xz}(\beta)+\sigma_{xz}(d)$ and $\sigma_{zz}(\vec{r}) = \sigma_{zz}(\alpha)+\sigma_{zz}(\beta)+\sigma_{zz}(d)$ as computed in Section II.

Let $L_{z\ min}$ be the minimum value of L_z obtained in optimal digitalization conditions, thus: $\alpha = 0°$, $\beta = 0°$ and $d = 170mm$. Let $L_{z\ ,max}$ be the maximum value of L_z obtained in extreme digitalization conditions, thus: $|\alpha| = 35°$, $|\beta| = 15°$ and $d = 240mm$.

We define the mean value of dispersion of a 3D cloud as: $\bar{L}_z = \frac{1}{n}\sum_{i=1}^{n} L_z(\vec{r}_i)$, with n the number of 3D points in the cloud.

Let t_s be a specified tolerance and t_m the measured deviation of a part under inspection. The deterministic inspection dictates that the part is in conformity with the specification if $t_m \leq t_s$. In nondeterministic inspection the result of the inspection must take into account the dispersion of the points used to carry out the tolerance control. We illustrate in Figure 5 the possible regions t_m can take in relation to t_s.

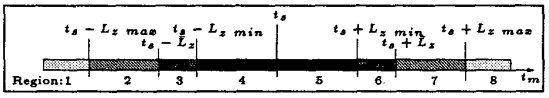

Fig. 5. Location of t_m related to t_s

The location of t_m related to t_s is used to quantify the result of the tolerance inspection by a qualitative value of reliability. In Table II we summarize the quantization of the inspection results according to the possible regions.

TABLE II
QUANTIZATION OF THE NONDETERMINISTIC INSPECTION RESULT

Region	Inspection result	Reliability value
1	Tolerance conform	very highly reliable
2	Tolerance conform	highly reliable
3	Tolerance conform	enough reliable
4	Tolerance conform	unreliable
5	Tolerance not conform	unreliable
6	Tolerance not conform	enough reliable
7	Tolerance not conform	highly reliable
8	Tolerance not conform	very highly reliable

The quantizations *enough reliable* and *unreliable* indicates that the inspection system is not sufficiently accurate to control the specified tolerance. Therefore it would be necessary either to improve the precision of the 3D data (to reduce $\bar{L}_z$ as much as possible), or to use another method of inspection.

V. INSPECTION RESULTS

We intend to check the specified tolerances in Figure 4 (so flatness, perpendicularity and angularity). In order to know the exact deviations of these tolerances,

we carried out the control with a CMM whom accuracy is $5\mu m$. We show the results in Table III with the tolerance under control, the value of specified tolerance (t_s), the measured value (t_m) and the result of the inspection.

TABLE III
TOLERANCES INSPECTION USING THE CMM

Tol. name	Tol. specific.	Measu. value	Result
Flatness	$10\mu m$	$10.8\mu m$	Not conform
Perpend.	$400\mu m$	$39\mu m$	Conform
Angularity	$400\mu m$	$26\mu m$	Conform

Using the acquisition strategy for the digitalization process we know the α, β and d parameters and therefore we can compute $L_{z\ min}, L_{z\ max}$ and $\bar{L}_z$ and perform nondeterministic inspection (as presented in Section IV-D). Table IV shows nondeterministic inspection results.

The geometrical tolerances of perpendicularity and angularity were found in conformity with the specifications, with a reliability value scoring *very highly reliable*. The geometrical tolerance of flatness was found not-conform with the specification, with a reliability score *unreliable*. The reliability value *unreliable* is due to the small value of the specification ($10\mu m$), and consequently another method of tolerance inspection should be used.

TABLE IV
NONDETERMINISTIC TOLERANCE INSPECTION

Tolerance name	Result	Reliability value
Size tolerance	Conform	Very highly reliable
Flatness	Not conform	Unreliable
Perpendicularity	Conform	Very highly reliable
Angularity	Conform	Very highly reliable

VI. CONCLUSION

We have presented an inspection system for manufactured parts that uses high accuracy range data. The high accuracy range data is obtained by using an optimum 3D data acquisition strategy. We have defined and implemented a methodology to check geometric tolerances, using a cloud of 3D points and a CAD model of the part. The system first registers a cloud of 3D points with a CAD model of the part, and then segments the 3D points in different surfaces by using the IGES CAD model. From the CAD model we know the exact description of the part, so we can use the implemented methodology to make the inspection of parts with complex surfaces.

The precision of the 3D data obtained with a range sensor is improved by the use of an acquisition strategy. These high precision 3D data are particularly interesting when very fine inspection is required. The acquisition strategy allows us to introduce a reliability value to the inspection result, and thus carries out a nondeterminist inspection. This reliability value constitutes a decision-making aid for the acceptance or rejection of the part under control.

REFERENCES

[1] F. Blais, M. Rioux and J.A. Beraldin, "Practical considerations for a design of a high precision 3-D laser scenner system," in *SPIE Optomechanical and Electro-Optical Design of Industrial Systems*, Bellinghan, June 1988, pp. 225–246.

[2] G.H. Tarbox and S.N. Gottschlich, "Planning for complete sensor coverage in inspection," *Computer Vision and Image Understanding*, vol. 61, no. N° 1, pp. 84–111, January 1995.

[3] K.A. Tarabanis, R.Y. TSAI and K. ANIL, "Computing occlusion-free viewpoints," *IEEE Transactions on Pattern Analysis and Machine Intelligence*, vol. 18, no. N° 3, pp. 279–292, March 1996.

[4] E. Trucco, M. Umasuthan, A.M. Wallace and V. Roberto, "Model-based planning of optimal sensor placements for inspection," *IEEE Transactions on Robotics and Automation*, vol. 13, no. 2, pp. 182–194, April 1997.

[5] F. Prieto, H.T. Redarce, P. Boulanger and R. Lepage, "CAD-based range sensor placement for optimum 3D data acquisition," in *Second International Conference on 3-D Digital Imaging and Modeling (3DIM'99)*, Ottawa, Canada, 4-8 October 1999, pp. 128–137.

[6] V. Moron, P. Boulanger, P. Masuda and H.T. Redarce, "Automatic inspection of industrial parts using 3-D optical range sensor," in *SPIE Proceedings, Videometrics IV*, 1995, vol. 2598, pp. 315–325.

[7] P.J. Besl and N.D. McKay, "A method for registration of 3-D shapes," *IEEE Transactions on Pattern Analysis and Machine Intelligence*, vol. 14, no. 2, pp. 239–256, February 1992.

[8] T.S. Newman and A.K. Jain, "A system for 3D CAD-based inspection using range images," *Pattern Recognition*, vol. 28, no. 10, pp. 1555–1574, 1995.

[9] F. Prieto, H.T. Redarce, R. Lepage and P. Boulanger, "A non contact CAD based inspection system," in *Quality Control by Artificial Vision*, Trois Rivières, Québec, Canada, 18-21 May 1999, pp. 133–138.

[10] V. Moron, P. Boulanger, H.T. Redarce, and A. Jutard, "Mise en correspondance du modèle CAO d'un objet avec son image 3D: Application à l'inspection," in *RFIA'96, Congrès de Reconnaissances de Formes et Intelligence Artificielle*, Rennes, France, 16-18 Janvier 1996, pp. 913–922.